BACCHUS

Impact of Biogenic versus Anthropogenic emissions on Clouds and Climate: towards a Holistic UnderStanding

Collaborative Project

SEVENTH FRAMEWORK PROGRAMME
ENV.2013.6.1-2

Atmospheric processes, eco-systems and climate change

Grant agreement no: 603445

Deliverable number:	**D4.1**
Deliverable name:	ESMs upgraded with new formulations for the emissions of organics and an improved treatment of BVOC-aerosol interactions and processes
WP number:	4
Delivery date:	Project month 18 (31/05/2015)
Actual date of submission:	31/05/2015
Dissemination level:	PU
Lead beneficiary:	KIT
Responsible scientist/administrator:	Almut Arneth
Estimated effort (PM):	40
Contributor(s):	Risto Makkonen (UHEL), Jón Egill Kristjánsson (UiO), Stijn Hantson (KIT), Kari Alterskjær (UiO), Ari Laaksonen (FMI) , Zak Kipling (UOXF)
Estimated effort contributor(s) (PM):	UHEL: 20PM, KIT: 12PM, UiO:7PM, FMI:1PM
Internal reviewer:	Jón Egill Kristjánsson

Summary of results

1. Emissions of organic aerosols and precursors in Earth System Models

1.1 Marine organic emissions (UHEL, UiO)

The recent sea-spray aerosol flux parameterization by Ovadnevaite et al. (2014) was implemented in the MPI-ESM (ECHAM5.5-HAM-SALSA) by Partanen et al. (2014). Wave height is not a diagnostic variable in ECHAM, hence the wind-generated wave height was obtained from ECMWF 6-hourly reanalysis dataset. Ovadnevaite et al. (2014) is used for particle diameter from 30 nm to 6 µm, and the size distribution shape from Monahan (1986) is applied for particle diameters from 6 to 10 µm but matching the flux to Ovadnevaite et al. (2014). The mass fraction of organic matter is calculated from chlorophyll a concentration and wind speed

$$f_{PMOM} = (0.569 \times c_{Chl\,a}) + (-0.0464 \times u_{10\,m} + 0.409)$$

Figure 1 shows the simulated emission of primary marine organic matter. The simulated global emission was found to be 1.1 Tg yr-1 (ranging from 0.5 to 1.8 Tg yr-1), which is in the lower part of the range 0.1-11.9 Tg yr-1 found by Gantt et al. (2012). The lack of wave height in BACCHUS ESMs reduces the feasibility of the above parameterization in ESM mode, however, present-day and hindcast simulations with ECMFW data are possible. Furthermore, ESM simulations can be extended to pre-industrial or future timescales with the assumption of a climatological wave height.

NorESM1 includes emission of 8 Tg yr-1 primary marine organic aerosol, based on Spracklen et al. (2008). This emission is distributed according to AeroCom fine mode sea salt emission. In NorESM2, which will be used in the BACCHUS production runs, the primary marine organic aerosol will be a linear function of the emission of the smallest sea salt mode (median dry radius of 0.022um). (The size of the annual emission and the constant determining the size relative to sea salt are not yet finalized, but will differ from NorESM1.)

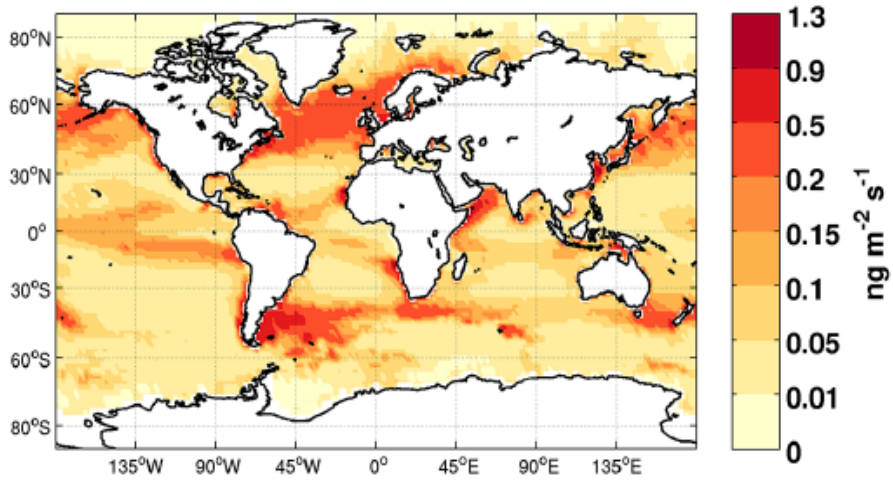

Figure 1. Emission of primary marine organic matter (PMOM) simulated by ECHAM with the Ovadnevaite et al. (2014) parameterization. Figure from Partanen et al. (2014).

Although marine BVOC emission flux could even exceed 10 Tg yr-1 (Shaw et al., 2010), the emissions are poorly constrained and have not been implemented in BACCHUS models so far.

1.2 Terrestrial BVOC emissions (KIT, UHEL)

1.2.1 BVOC model frameworks

Current studies on the atmospheric impact studies of BVOC´s are overwhelmingly based on the MEGAN model (Guenther et al., 1995; Guenther et al., 2012). The Model of Emissions of Gases and Aerosols from Nature version 2.1 (MEGAN2.1) is an empirically-derived model for estimating fluxes of biogenic compounds. It includes the main variables currently known to drive BVOC emissions (temperature, solar radiation, leaf area index etc.). MEGAN2.1 gives estimates for isoprene, 40+ monoterpene species and 30+ Sesquiterpene species.

The BVOC module in LPJ-GUESS is an alternative (semi-)process-based approach, linking emissions to the photosyntethic activity of the vegetation. The BVOC emission module combines the process-based leaf level emission model from Niinemets et al. (2002; 1999) with the LPJ-GUESS vegetation model as described in Arneth et al. (2007) for isoprene and Schurgers et al. (2009) for monoterpenes.
Within the BACCHUS project, a speciation of the monoterpene emission has been implemented, accounting for the main 8 species, together with a "rest-monoterpene" group. Both changes in emission factors as storage fraction for each species are taken into account (see Deliverable 2.1). LPJ-GUESS will provide offline-emission fields for all BACCHUS-ESMs as an alternative to the predominant MEGAN implementations. The implemented monoterpene speciation furthermore allows for distinct lumping methods for monoterpenes before emitting to the atmosphere-module, taking into account different SOA-formation potential of different species. This is especially important considering the changing fraction of the different monoterpene species emitted over time. In figure 2 the monoterpene emissions for 3 species over the last century are given, with different temporal trends between the different monoterpene species.

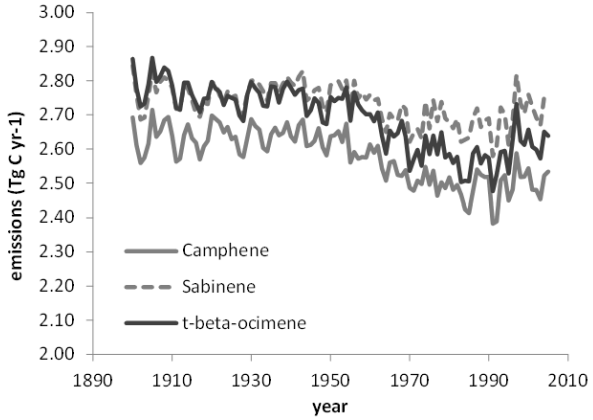

Figure 2. Global annual emissions of three monoterpene species over the last century (1900-2005) from LPJ-GUESS forced with CRU climate data and without considering land-use change.

Isoprene and monoterpene emissions are not well resolved at the global scale (Arneth et al. 2008). While total global isoprene emissions coincide well between the MEGAN2.1 and the LPJ-GUESS approach, large differences can be observed for monoterpenes. These discrepancies are present for both the total sum of monoterpenes and for the different monoterpene species (see Table 1), indicating the need to consider multiple BVOC emission estimates due to the existing uncertainty on the global budget of monoterpene emissions.

	isoprene	mono terpenes	alfa-pinene	beta-pinene	sabinene	t-beta-ocimene	3-carene	camphene	limonene	myrcene	rest mono.
LPJ-GUESS	523	34.1	12.8	4.1	2.7	2.6	2.5	1.6	3.7	2.0	2.0
MEGAN2.1	535	157	66.1	18.9	9	19.4	7.1	4	11.4	8.7	17.7

Table 1. Comparison of the isoprene and monoterpene emissions (Tg yr-1) for the year 2000 from MEGAN2.1 and LPJ-GUESS (for details on LPJ-GUESS, see Deliverable 2.1).

1.2.2 BVOC emissions in ESM´s

BVOC emissions are treated in all ESM´s used in BACCHUS.

- HadGEM uses currently prescribed BVOC emissions from GEIA. For UKESM1 it is planned to coupled to the JULES land surface model. JULES introduced a photosynthesis-based biogenic isoprene emission scheme in version 3.2 as described by Pacifico et al. (2011).

Both MPI-ESM and NorESM include an interactive BVOC emission module based on the MEGAN framework.

- MPI-ESM can calculate BVOC emissions interactively in MEGAN algorithm in the HAM-module. Isoprene and monoterpene emissions can also be estimated by the JSBACH vegetation model within MPI-ESM.
- NorESM can calculate BVOC emissions interactively in Community Land Model CLM2 (MEGAN algorithm). NorESM2 is now running with CLM4.0, but CLM4.5 is the goal before the end of the year.

As an alternative to these MEGAN-based implementations, both MPI-ESM and NorESM can use prescribed BVOC emissions, calculated off-line by LPJ-GUESS.

Figure 3 shows summer monoterpene emissions simulated by several BACCHUS models. The monoterpene emission algorithm implemented in MPI-ESM/JSBACH results in the lowest emissions globally. The MEGAN1 implementation in NorESM/CLM results in relatively similar emission patterns in the Northern Hemisphere as MEGAN2.1 driven with MERRA (Modern Era-Retrospective Analysis For Research and Applications) meteorological fields, but NorESM simulates distinctively lower emission in the tropics. The monoterpene emissions simulated by LPJ-GUESS are generally more evenly spread. These differences, both in magnitude and spatial heterogeneity are in line with the current day uncertainty in magnitude and distribution of global monoterpene emissions (e.g. Arneth et al., 2008). KIT and UHEL are planning to coordinate a BACCHUS activity on thorough evaluation of BVOC emissions in BACCHUS models.

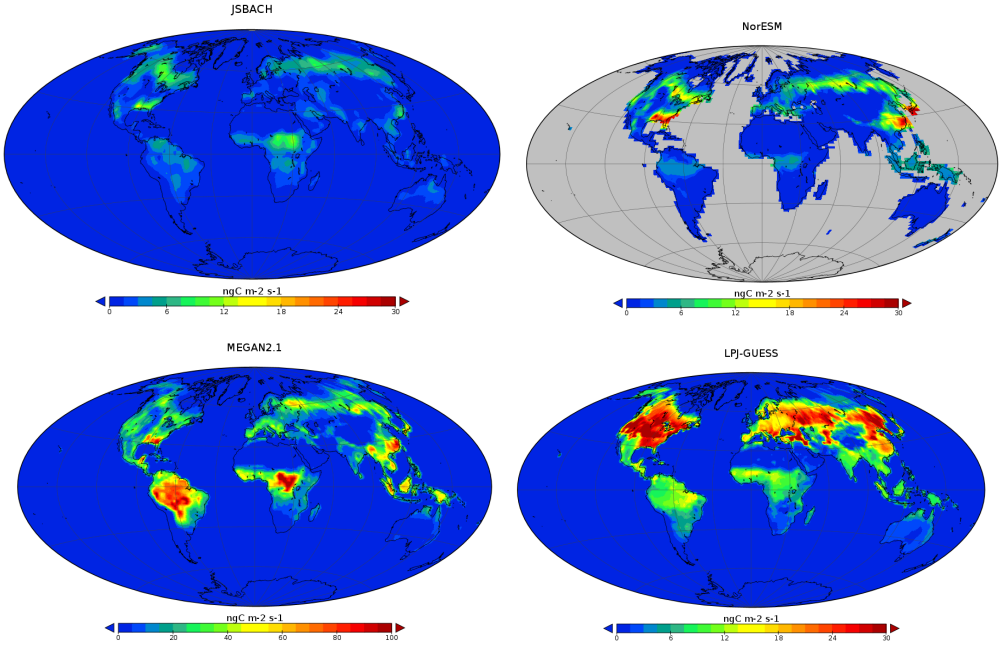

Figure 3. July monoterpene emission flux simulated by MPI-ESM (JSBACH), NorESM (CLM), MEGAN2.1 and LPJ-GUESS.

To demonstrate the response of interactive BVOC emissions to changing climate conditions, NorESM was simulated under present-day and doubled CO_2 concentrations. The experiments were performed with a slab-ocean model and the model was integrated for 60 years. The doubling of CO_2 led to an increase of 2-meter temperature by ~3.3 K. The simulated climate change increased monoterpene emissions from present-day value 76 TgC/year to 100 TgC/year, corresponding to a 30% increase (Figure 4). The response is in line with earlier findings by Heald et al. (2008) and Liao et al. (2006), who found an increase of 19% (+1.8 K) and 58% (+4.8 K) in monoterpene emission (temperature increase), respectively.

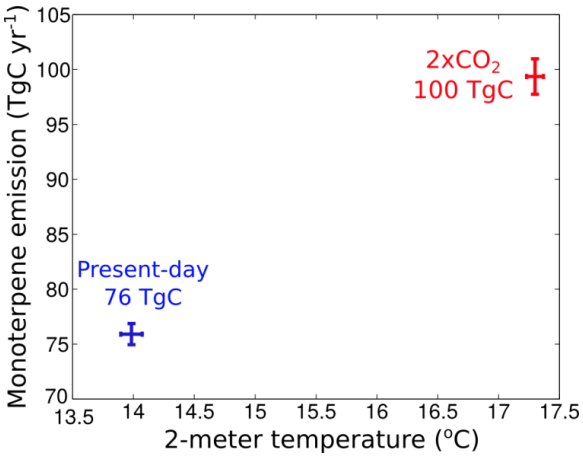

Figure 4. Response of NorESM/CLM monoterpene emission to climate change under doubled CO2 simulation. Data is averaged over simulation years 30-60. NorESM is run with slab ocean configuration, and values of 76 and 100 TgC indicate emissions at equilibrium. Error bars indicate one standard deviation.

1.3 Fire emissions (KIT, UHEL)

1.3.1 LPJ-GUESS-SIMFIRE

A simple but non-linear model of fractional burned area was developed by Knorr et al. (2014), optimized against observed burned-area products. The module SIMFIRE predicts fractional area burned per fire season and does not model ignitions explicitly, but uses empirical factors to predict burned area. This empirical equation includes the main drivers of fires globally, namely vegetation, climate and human impact. The presence of vegetation is documented by FAPAR (fraction of absorbed photosynthetically active radiation), a radiation-based quantity that is both easy to observe from satellites and modeled by vegetation models. The presence of vegetation by itself indicates two things relevant to the probability of fire: the accumulation of fuel as dead plant matter derived from plant matter production, and the continuity of the vegetation cover, which strongly influences fire spread. Fuel load and fire spread themselves are not described explicitly.
The drought conditions necessary for fire occurrence are characterized by the use of the Nesterov index (Nesterov 1949; Venevsky et al. 2002; Thonicke et al. 2010), defined as:

$$N(t+\Delta t) = \begin{cases} N(t) + T_{max}(t)\,[T_{max}(t) - T_{min}(t) + 4\mathrm{K}] & \text{if } P(t)<3\ \mathrm{mm}, \end{cases}$$

$N(t)$ is the daily Nesterov index at time step t, Δt is one day, and T_{max} and T_{min} daily maximum and minimum temperature, respectively, and P daily precipitation. The offset of 4K is based on the assumption that the dew point temperature is four degrees below the minimum temperature. In this form, drought can be characterized without the need for humidity or surface wind speed data, both of which are extremely unreliable at large scales. This daily Nesterov index is then converted to monthly maximum values, N_m. N_m has two functions: it is used to determine the start and end of the average fire year for a given location, and the severity of drought during each particular fire year.
Human population density is used here as a surrogate for ignitions, active fire suppression, and fire suppression through landscape fragmentation or modification.

Finally, the model allows differentiation by the main broad land cover categories summarized from the IGBP (International Geosphere Biosphere Programme) land cover classes (Friedl et al. 2002), easily defined based on vegetation model parameters.

The annual burned-area model computes fractional area burned for a fixed fire year ending in the month with the lowest maximum Nesterov index according the following equation:

$$A(y) = a(L)\, F^{b}\, N_{max}(y)^{c} \,/\, [1 + \exp(d + ep)]$$

A is the fractional area burned of the grid cell, y the fire year, L land cover class (1–8), F the interannual average of annual maximum of monthly FAPAR, N_{max} annual maximum Nesterov index, p population density in people/km^2. b, c, d and e are global, and $a(L)$ eight regional tunable parameters.

Here, the impact of population density on fire is formulated using a logistic function modified by two parameters. This formulation does not incorporate any prior knowledge about the impact of humans on fire occurrence. The model is optimized against the Global Fire Emissions Database version 3 (GFED3)

satellite based burned area dataset (Giglio et al., 2013). The annual burned area is calculated on a monthly basis depending on the seasonality of the fire occurrence prescribed for each grid cell, extracted from GFED3.1 burned area data and considered invariant between years.

Fuel combustion depends on the fuel type, with 100% of the grass and fine fuel combusted. Woody litter has a combustion factor of 20%. Tree mortality depends on the fireline intensity and flame height, implemented following Thonicke et al. (2010) and computed from rate of spread and fuel consumed using Byram's equation (Byram 1959). Moreover, SIMFIRE is currently merged with the latest version of LPJ-GUESS, including a coupled carbon-nitrogen cycle (Smith et al., 2014), which will then allow to assess interactions of global environmental changes (climate, CO_2, land-use, N deposition) with vegetation and fire dynamics, and the related fire aerosol and trace gas emissions.

The primary output of LPJ-GUESS-SIMFIRE is the total emitted carbon for each grid cell (see figure 5 for an example for the year 2000). These total carbon emissions are then converted to emissions of different species following the Plant Functional Type specific emissions factors based on an updated version of the Andreae and Merlet (2001) dataset. Applying emission factors allows, in principle, also to investigate emission changes (e.g., in aerosol) due to changing burn-conditions, as demonstrated by Knorr et al. (2012).

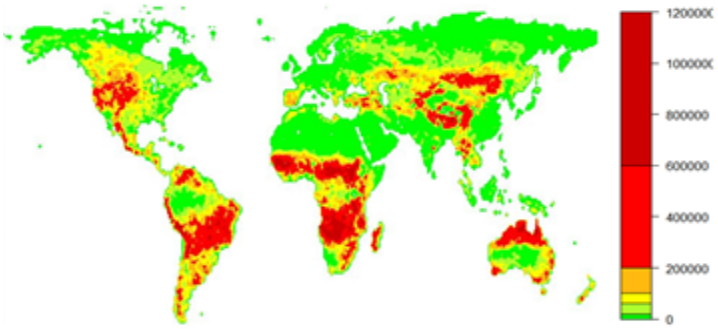

Figure 5. Total C emissions (T C yr-1) by fire for the year 2000 as simulated by LPJ-GUESS-SIMFIRE.

1.3.2 Implementation of fire emissions in ESM

The fire emissions simulated by LPJ-GUESS-SIMFIRE have been implemented in ECHAM5.5-HAM2 (MPI-ESM). The original GFED emission inventory for SO_2, BC and OC was replaced by those from LPJ-GUESS in a short simulation conducted to test the implementation. Figure 6 shows simulated July concentrations of organic carbon, and differences in CCN(1.0%) concentration between GFED inventory and LPJ-GUESS. Initial tests indicate enhanced emissions in Africa between 0°S and 30°S and in parts of the Northern hemisphere high latitudes. However, the simulations compare 2009 fire emissions from LPJ-GUESS-SIMFIRE to climatological emissions from GFED, which probably contribute to the differences seen. UHEL and KIT will continue to further implement LPJ-GUESS emissions from different years to MPI-ESM, allowing more stringent evaluation of impacts on aerosols and climate. Furthermore, KIT and UHEL will address the changes in fire aerosol climate forcing since pre-industrial.

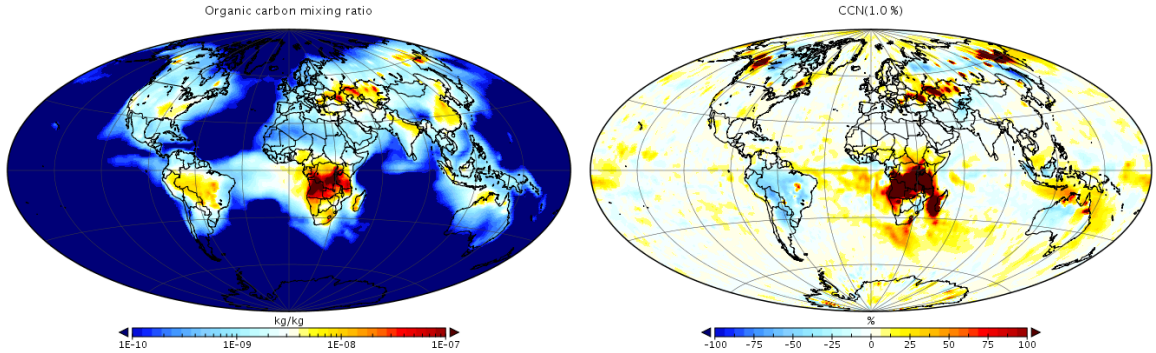

Figure 6. Organic carbon mixing ratio simulated by ECHAM5.5-HAM2 with LPJ-GUESS-SIMFIRE fire emissions (left panel) and relative difference in CCN(1.0%) concentration between LPJ-GUESS and original GFED emission inventory (right panel), red indicating higher CCN concentrations with LPJ-GUESS emissions. Results are shown for simulated July.

1.3.3 Emission height

One of the main factors determining the longevity of the emitted aerosols is the emission or injection plume height. Emission height can be modeled based on atmospheric conditions and fire characteristics, mainly the energy released by the fire. Multiple models have recently been developed, with semi-empirical equations based on the fire radiative power giving good results (e.g. Sofiev et al., 2012, Viera et al., 2015). Within LPJ-GUESS-SIMFIRE the fire line intensity, which indicates the energy released by the fire, is estimated and given as an extra variable and therefore the emission height could be estimated. However, an adaptation of current emission height parameterizations, relying on Fire Radiative Power (FRP) estimated from satellites, is needed to relate FRP and modelled fire line intensity, which is currently in progress.

1.4 PBAP emissions (UHEL,UiO)

The numbers of primary biological aerosol particles (PBAP) are generally too low to influence cloud condensation nuclei concentrations significantly, but PBAP are efficient ice nuclei. Spracklen and Heald (2014) showed that PBAP contributed regionally less than 1% in CCN concentrations. Hoose et al. (2010a) and Sesartic et al. (2012) implemented bacterial emissions in NorESM and ECHAM5-HAM/MPI-ESM, respectively, coupling PBAP to the ice nucleation module. In both studies, global cloud effects of bacteria were found to be small, with some pronounced influence in liquid water path (LWP)/ice water path (IWP) in boreal regions reported by Sesartic et al. (2012). In NorESM, an updated version of the Hoose et al. (2010b) ice nucleation scheme (Wang et al., 2014) is currently being tested. The work by Spracklen and Heald (2014) done with the Global Model of Aerosol Processes (GLOMAP-mode) is expected to be included in the UKESM/HadGEM used in BACCHUS. Ice nucleation is the focus of BACCHUS deliverable D4.2 (M36).

2. Improved treatment of BVOC-aerosol interactions and processes

Due to inherently distinct aerosol-chemistry implementations in the BACCHUS ESMs, the approaches to organic aerosols and chemistry are rather different. However, BACCHUS-groups have pursued joint development and efficient sharing of developed modules and parameterizations.

2.1 MPI-ESM (UHEL)

2.1.1 Stabilized Criegee intermediates

Sipilä et al. (2014) investigated the importance of stabilized Criegee intermediates (sCI) in atmospheric oxidation, specifically SO_2 oxidation. The stabilized Criegee intermediates can form by e.g. ozonolysis of isoprene and monoterpenes. The sCI oxidation mechanism has been included in MPI-ESM (specifically ECHAM5.5-HAM2), and the mechanism has been tested with two simulation experiments. Monoterpene emissions in these experiments were prescribed according to Guenther et al. (1995). The model was integrated for 16 months, and the last 12 months were used for the analysis. The model meteorological fields were nudged towards ERA40 re-analysis data for the year 2001 in all simulations. The model included 31 levels in the vertical and used T42 horizontal resolution, corresponding to a horizontal grid of approximately 2.8°. Two simulations were performed with both present-day and future aerosol and precursor emissions. The control simulation ("CTRL") included SO_2 oxidation both by the hydroxyl radical in the gas phase, and by H_2O_2 and O_3 in the aqueous phase. The second simulation ("SCI") included the additional SO_2 oxidation pathway by stabilized Criegee-intermediates in the gas phase. The SO_2 oxidation pathway by stabilized Criegee-intermediates was implemented in the model. The model sCI production was set to match the measured (Mauldin et al., 2012) concentrations of sCI in Hyytiälä boreal forest site and sCI lifetime was assumed to be constant.

Preliminary results showed that SO_2 oxidation by sCI increased H_2SO_4 concentrations in the continental boundary layer (Figure 7). The difference in sulphuric acid concentration is a function of both SO_2 available for oxidation and monoterpene emissions. Figure 7 shows that in a few low-SO_2 areas, such as South America, Central Africa and a band from Europe to Siberia, the relative increase in sulphuric acid concentration can be significant. The tropical regions in South America and Africa show a fairly constant increase in sulphuric acid throughout the year, ranging from a few percent up to 30%. Northern mid and high latitudes show a strong seasonal variation, stemming e.g. from variation in monoterpene emissions and photochemical activity (it should be noted that unlike wild-fire SO_2 emissions, the prescribed anthropogenic SO_2 emissions do not contain intra-annual variation). Even annually averaged, the increase in sulphuric acid concentration can be up to 50% in Northern South America, 5-15% in Northern Eurasia and 5-30% in North America.

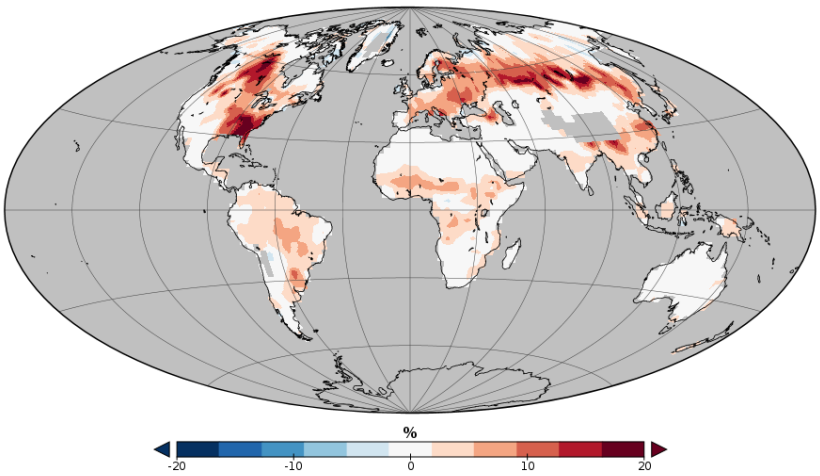

Figure 7. Increase in sulfuric acid concentration due to additional sCI-oxidation mechanism, as opposed to original chemical mechanisms in ECHAM5.5-HAM2 (OH, H_2O_2, O_3).

2.1.2 New SOA formation module accounting for ELVOCs

A new secondary organic aerosol (SOA) module accounting for Extremely Low-Volatility Organic Compounds (ELVOCs) was developed for ECHAM5-HAM in MPI-ESM (Figure 8). A hybrid SOA model has been developed for the aerosol microphysics model M7 in MPI-ESM to include both kinetic condensation to Fuchs-corrected surface area (Andrea et al., 2013) and partitioning according to pre-existing organic mass (Jokinen et al., 2015). Three gas-phase tracers were included for BVOCs: isoprene, endocyclic and other monoterpenes. All three simulated BVOC tracers produce both Extremely Low-Volatility Organic Compounds (ELVOCs) and Semi-Volatile Organic Compounds (SVOCs). While tracers are implemented for BVOCs, oxidation products are partitioned to the aerosol phase immediately. ELVOCs are assumed to condense on the particle-phase according to surface area, while SVOCs are partitioned according to organic mass in each mode. No evaporation to the gas-phase is included for any SOA product, hence SVOCs are simulated effectively as non-volatile LVOCs. Several monoterpene compounds can be lumped in respective categories. Included endocyclic monoterpenes are α-pinene, limonene, α-phellandrene, β-phellandrene, 3-carene, terpinolene, α-terpinene and γ-terpinene. Considered monoterpenes in the "other monoterpenes" group are e.g. camphene, β-pinene, myrcene and t-β-ocimene. Global annual emissions from MEGAN2.1 are presented in Table 2, highlighting the importance of specific species in terms of global mass emission. Currently, a total SOA yield of 15% from monoterpenes and 5% from isoprene is assumed. Laboratory measurements are used to constrain ELVOC yields from all precursor reactions (isoprene, monoterpenes) so that ELVOC yields and SOA formation can be extended to cover sesquiterpenes and anthropogenic compounds when more information becomes available.

Separating the condensational behaviour of SVOCs/LVOCs and ELVOCs improves the SOA module in terms of size distribution effects, but neglects the effects of true semi-volatile part of SOA. A gas-aerosol partitioning scheme could be added on top of the above scheme with some additional tracers and added computational cost. The SOA module would not consider certain potentially important features of SOA formation, including

- Multi-phase SOA formation
- Effect of NOx on SOA yield
- Evaporation of primary OA, potential further oxidation in gas-phase

Generally the model is expected to underestimate both the global amount of SOA formed and the anthropogenic influence on SOA formation. However, the model is intended to capture the main features of coupling between anthroposphere, biosphere, CCN and cloud forcing (Jokinen et al., 2015). Furthermore, the module is developed specifically for ESM purposes by minimizing the computational costs allowing for centennial integrations of the models.

Further development of MPI-ESM secondary organic aerosol module will continue with BACCHUS and with external contributions, potentially covering some of the abovementioned drawbacks of the current implementation.

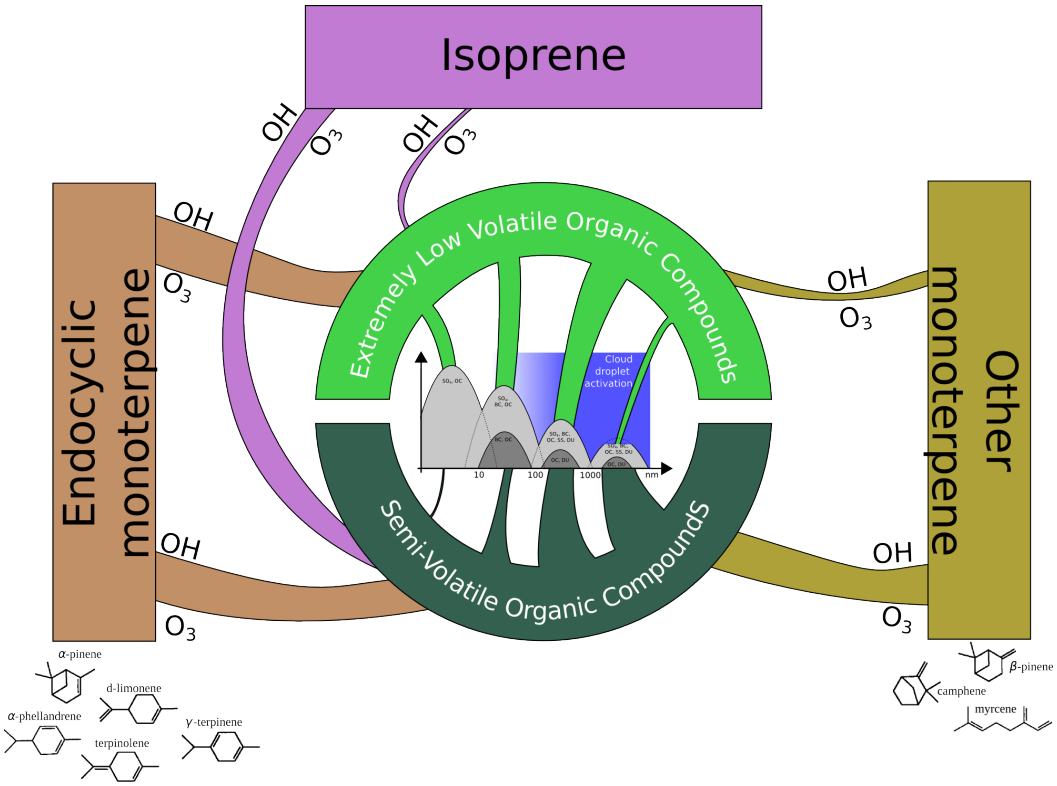

Figure 8. Schematic of the hybrid SOA formation module in MPI-ESM, grouping monoterpenes to endocyclic and other compounds. In the diagram, NO_3 is a sink for precursors, but does not result in SOA formation. ELVOCs (light green) condense according to Fuchs-corrected surface area, SVOCs (LVOCs) according to organic mass.

2.2 NorESM (UiO, UHEL)

NorESM1 (Kirkevåg et al., 2013) included a simplified approach for nucleation of new particles, and secondary organic aerosol formation was described by primary aerosol emission of 37.5 Tg yr-1 (scaled

from 19.1 Tg yr-1 in Guenther et al., 1995). In Makkonen et al. (2014), the description of organic aerosol was reformulated.

Makkonen et al. (2014) implemented emissions of monoterpene and isoprene to NorESM1. These SOA precursors are oxidized by OH, O_3 and NO_3. A certain fraction of the oxidation products is assumed low-volatile enough to either nucleate or condense on nucleation-sized particles. The remainder of the formed SOA is placed in the original "SOA-mode" of NorESM1. Organic nucleation is implemented according to several semi-empirical parameterizations from Paasonen et al. (2010), e.g.

$$J_2 = A_{S1}[H2SO4] + A_{S2}[ORG],$$

where [ORG] is the concentration of nucleating organic vapour. After nucleation, particles grow further by condensation of sulfuric acid and organic vapours. The subsequent growth is described following Lehtinen et al. (2007). The transition rate is determined by the concentration of sulfuric acid and organic vapors available for condensational growth and by the coagulation sink of the newly formed 1-2 nm particles onto preexisting aerosols.

The organic vapors available for this transition have been found to be very important for the growth of atmospheric particles (Riipinen et al., 2011; Keskinen et al., 2013). In this model extension, these organic vapors result from a new treatment of biogenic precursors in the model. In the standard model version NorESM1-M (Kirkevåg et al., 2013), SOA was prescribed as a monthly surface source. Now, emissions of monoterpenes and isoprenes are oxidized by O_3, OH and NO_3 to form low and semi-volatile organic vapors with yields of 15% and 5%, respectively. It is assumed that 50 % of the monoterpene ozonolysis products are of low enough volatility that they can contribute to the condensational growth of the newly nucleated particles, while the rest of the oxidized organic vapors is assumed to condensate onto preexisting aerosols and is lumped together with organic carbon from biomass burning, fossil fuel and marine organic emissions. In NorESM1 isoprene emissions were not allowed to form SOA, while this is not the case for the current version of NorESM2. NorESM1 did not hold a tracer for organic mass in nucleation mode and the nucleated particles were considered to consist of sulfate. In NorESM2 this is no longer the case and separate tracers for nucleation and accumulation mode SOA are included in the model.

The main advantages of the new treatment of SOA formation are that the atmospheric composition influences the SOA size distribution and particle number; that SOA is now allowed to form outside the boundary layer and that, with interactive BVOC emissions, we can conduct studies of the effects of a changing climate on SOA formation and following feedbacks.

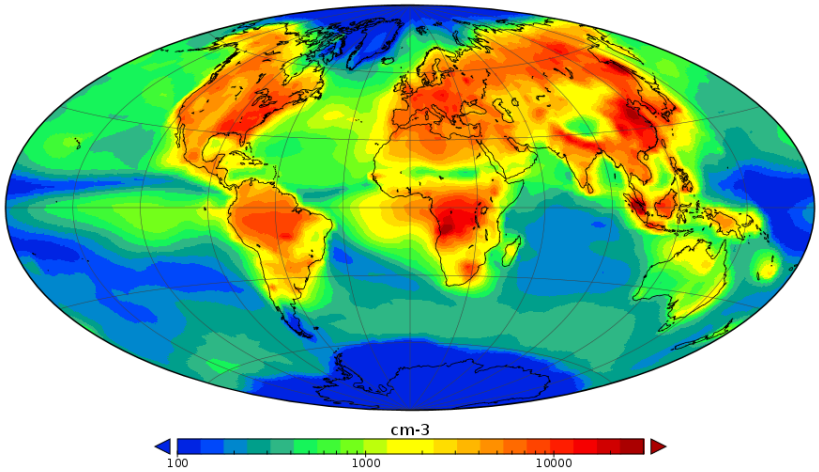

Figure 9. Aerosol number concentration in July with organic nucleation simulated by NorESM1. The effect of biogenic emissions is clearly visible at e.g., Eurasian high latitudes.

2.3 HadGEM/UKESM (UOXF)

The Hadley Centre Global Environmental Model (HadGEM) versions 1-2 include a mass-based aerosol scheme (CLASSIC). The mass-based scheme was used for CMIP5 simulations in the Earth System version HadGEM2-ES. Current integration of HadGEM and UKCA will establish modal aerosol module GLOMAP-mode in the Earth System version UKESM.

GLOMAP-mode (Mann et al., 2010) includes four main aerosol species: sulphate, black carbon, organic carbon and sea salt. The model describes aerosols with five modes, while organic carbon is considered in soluble Aitken, accumulation and coarse modes, and the insoluble Aitken mode. GLOMAP-mode does include mineral dust and, although current configurations of HadGEM use a separate dust scheme, GLOMAP-mode dust is expected to be used in UKESM1. When dust is switched on, there are seven modes, much as in ECHAM-HAM (using M7). Nitrate has been implemented as well, although evaluation and integration into the latest model version is ongoing it is expected to be in UKESM1. GLOMAP-mode includes monoterpenes as a tracer compound. Monoterpenes are oxidized by ozone as well as hydroxyl and nitrate radicals. SOA is condensing on aerosol modes according to adjusted condensation sink.

Bibliography

Andreae, M. O., and Merlet, P.: Emission of trace gases and aerosols from biomass burning, Glob. Biogeochem. Cycle, 15, 955-966, 2001.

Arneth, A., Niinemets, U., Pressley, S., Back, J., Hari, P., Karl, T., Noe, S., Prentice, I. C., Serca, D., Hickler, T., Wolf, A., and Smith, B.: Process-based estimates of terrestrial ecosystem isoprene emissions: Incorporating the effects of a direct co2-isoprene interaction, Atmos. Chem. Phys., 7, 31-53, 2007.

Arneth, A., Monson, R. K., Schurgers, G., Niinemets, U., and Palmer, P. I.: Why are estimates of global terrestrial isoprene emissions so similar (and why is this not so for monoterpenes)?, Atmos. Chem. Phys., 8, 4605-4620, 2008.

Byram, G. M.: Combustion of forest fuels, in: Forest fire: Control and use, edited by: Davis, K. P., McGraw-Hill, New York, 155-182, 1959.

D'Andrea, S. D., Häkkinen, S. A. K., Westervelt, D. M., Kuang, C., Levin, E. J. T., Kanawade, V. P., Leaitch, W. R., Spracklen, D. V., Riipinen, I., and Pierce, J. R.: Understanding global secondary organic aerosol amount and size-resolved condensational behavior, Atmos. Chem. Phys., 13, 11519-11534, doi:10.5194/acp-13-11519-2013, 2013.

Gantt, B., Johnson, M. S., Meskhidze, N., Sciare, J., Ovadnevaite, J., Ceburnis, D., and O'Dowd, C. D.: Model evaluation of marine primary organic aerosol emission schemes, Atmos. Chem. Phys., 12, 8553–8566, doi:10.5194/acp-12-8553-2012, 2012.

Giglio, L., Randerson, J. T., and Werf, G. R.: Analysis of daily, monthly, and annual burned area using the fourth-generation global fire emissions database (gfed4), Journal of Geophysical Research: Biogeosciences, 2013.

Guenther, A., Hewitt, C. N., Erickson, D., Fall, R., Geron, C., Graedel, T., Harley, P., Klinger, L., Lerdau, M., McKay, W. A., Pierce, T., Scholes, B., Steinbrecher, R., Tallamraju, R., Taylor, J., and Zimmerman, P.: A global model of natural volatile organic compound emissions, Journal of Geophysical Research: Atmospheres, 100, 8873-8892, 10.1029/94jd02950, 1995.

Guenther, A. B., Jiang, X., Heald, C. L., Sakulyanontvittaya, T., Duhl, T., Emmons, L. K., and Wang, X.: The model of emissions of gases and aerosols from nature version 2.1 (megan2.1): An extended and updated framework for modeling biogenic emissions, Geosci. Model Dev., 5, 1471-1492, 10.5194/gmd-5-1471-2012, 2012.

Hoose, C., Kristjánsson, J. E., and Burrows, S. M.: How important is biological ice nucleation in clouds on a global scale?, Environmental Research Letters, 5, 024009, 2010a.

Hoose, C., J. E. Kristjánsson, J.-P. Chen, and A. Hazra, 2010b: A classical-theory-based parameterization of heterogeneous ice nucleation by mineral dust, soot and biological particles in a global climate model. *J. Atmos. Sci., 67*, 2483-2503.

Houghton, R., Hobbie, J., Melillo, J. M., Moore, B., Peterson, B., Shaver, G., and Woodwell, G.: Changes in the carbon content of terrestrial biota and soils between 1860 and 1980: A net release of CO2 to the atmosphere, Ecological Monographs, 53, 235-262, 1983

Jokinen, T., Berndt, T., Makkonen, R., Kerminen, V.-M., Junninen, H., Paasonen, P., Stratmann, F., Herrmann, H., Guenther, A., Worsnop, D.R., Kulmala, M., Ehn, M. and Sipilä, M.: Production of extremely low-volatile organic compounds from biogenic emissions: measured yields and atmospheric implications, published ahead of print May 26, 2015, doi:10.1073/pnas.1423977112, 2015.

Keskinen, H., and co-authors, 2013: Evolution of particle composition in CLOUD nucleation experiments. Atmos. Chem. Phys., 13, 5587-5600.

Kirkevåg, A., Iversen, T., Seland, Ø., Hoose, C., Kristjánsson, J. E., Struthers, H., Ekman, A. M. L., Ghan, S., Griesfeller, J., Nilsson, E. D., and Schulz, M.: Aerosol–climate interactions in the Norwegian Earth System Model – NorESM1-M, Geosci. Model Dev., 6, 207-244, doi:10.5194/gmd-6-207-2013, 2013.

Kloster, S., Mahowald, N. M., Randerson, J. T., Thornton, P. E., Hoffman, F. M., Levis, S., Lawrence, P. J., Feddema, J. J., Oleson, K. W., and Lawrence, D. M.: Fire dynamics during the 20th century simulated by the community land model, Biogeosciences, 7, 1877-1902, 10.5194/bg-7-1877-2010, 2010.

Knorr, W., Lehsten, V., and Arneth, A.: Determinants and predictability of global wildfire emissions, Atmos. Chem. Phys., 12, 6845-6861, DOI 10.5194/acp-12-6845-2012, 2012

Knorr, W., Kaminski, T., Arneth, A., and Weber, U.: Impact of human population density on fire frequency at the global scale, Biogeosciences, 11, 1085-1102, 10.5194/bg-11-1085-2014, 2014.

Lehtinen, K. E. J., M. Dal Maso, M. Kulmala, and V.-M. Kerminen, 2007: Estimating nucleation rates from apparent particle formation rates and vice versa: Revised version of the Kerminen-Kulmala equation. J. Aerosol Sci., 38, 988-994.

Mann, G. W., Carslaw, K. S., Spracklen, D. V., Ridley, D. A., Manktelow, P. T., Chipperfield, M. P., Pickering, S. J., and Johnson, C. E.: Description and evaluation of glomap-mode: A modal global aerosol microphysics model for the ukca composition-climate model, Geosci. Model Dev., 3, 519-551, 10.5194/gmd-3-519-2010, 2010.

Monahan, E. C., Spiel, D. E., and Davidson, K. L.: A model of marine aerosol generation via whitecaps and wave disruption, in: Oceanic Whitecaps and their Role in Air–Sea Exchange, edited by: Monahan, E. C. and MacNiocaill, G., D. Reidel, Norwell, Mass., 167–174, 1986.

Niinemets, Ü., Tenhunen, J. D., Harley, P. C., and Steinbrecher, R.: A model of isoprene emission based on energetic requirements for isoprene synthesis and leaf photosynthetic properties for liquidambar and quercus, Plant, Cell & Environment, 22, 1319-1335, 10.1046/j.1365-3040.1999.00505.x, 1999.

Niinemets, Ü., Seufert, G., Steinbrecher, R., and Tenhunen, J. D.: A model coupling foliar monoterpene emissions to leaf photosynthetic characteristics in mediterranean evergreen quercus species, New Phytol., 153, 257-275, 10.1046/j.0028-646X.2001.00324.x, 2002.

Ovadnevaite, J., Manders, A., de Leeuw, G., Ceburnis, D., Monahan, C., Partanen, A.-I., Korhonen, H., and O'Dowd, C. D.: A sea spray aerosol flux parameterization encapsulating wave state, Atmos. Chem. Phys., 14, 1837–1852, doi:10.5194/acp-14-1837-2014, 2014.

Paasonen, P., Nieminen, T., Asmi, E., Manninen, H. E., Petäjä, T., Plass-Dülmer, C., Flentje, H., Birmili, W., Wiedensohler, A., Hõrrak, U., Metzger, A., Hamed, A., Laaksonen, A., Facchini, M. C., Kerminen, V.-M., and Kulmala, M.: On the roles of sulphuric acid and low-volatility organic vapours in the initial steps of atmospheric new particle formation, Atmos. Chem. Phys., 10, 11223-11242, doi:10.5194/acp-10-11223-2010, 2010.

Partanen, A.-I., Dunne, E. M., Bergman, T., Laakso, A., Kokkola, H., Ovadnevaite, J., Sogacheva, L., Baisnée, D., Sciare, J., Manders, A., O'Dowd, C., de Leeuw, G., and Korhonen, H.: Global modelling of direct and indirect effects of sea spray aerosol using a source function encapsulating wave state, Atmos. Chem. Phys., 14, 11731-11752, doi:10.5194/acp-14-11731-2014, 2014.

Pacifico, F., Harrison, S. P., Jones, C. D., Arneth, A., Sitch, S., Weedon, G. P., Barkley, M. P., Palmer, P. I., Serça, D., Potosnak, M., Fu, T. M., Goldstein, A., Bai, J., and Schurgers, G.: Evaluation of a photosynthesis-based biogenic isoprene emission scheme in jules and simulation of isoprene emissions under present-day climate conditions, Atmos. Chem. Phys., 11, 4371-4389, 10.5194/acp-11-4371-2011, 2011.

Riipinen, and co-authors, 2011: Organic condensation: a vital link connecting aerosol formation to cloud condensation nuclei (CCN) concentrations. Atmos. Chem. Phys., 11, 3865-3878.

Schurgers, G., Arneth, A., Holzinger, R., and Goldstein, A. H.: Process-based modelling of biogenic monoterpene emissions combining production and release from storage, Atmos. Chem. Phys., 9, 3409-3423, 2009.

Sesartic, A., Lohmann, U., and Storelvmo, T.: Bacteria in the ECHAM5-HAM global climate model, Atmos. Chem. Phys., 12, 8645-8661, doi:10.5194/acp-12-8645-2012, 2012.

Smith, B., Wårlind, D., Arneth, A., Hickler, T., Leadley, P., Siltberg, J., and Zaehle, S.: Implications of incorporating n cycling and n limitations on primary production in an individual-based dynamic vegetation model, Biogeosciences, 11, 2027-2054, 10.5194/bg-11-2027-2014, 2014.

Sofiev, M., Ermakova, T., and Vankevich, R.: Evaluation of the smoke-injection height from wild-land fires using remote-sensing data, Atmos. Chem. Phys., 12, 1995-2006, 2012.

Sipilä, M., Jokinen, T., Berndt, T., Richters, S., Makkonen, R., Donahue, N. M., Mauldin III, R. L., Kurtén, T., Paasonen, P., Sarnela, N., Ehn, M., Junninen, H., Rissanen, M. P., Thornton, J., Stratmann, F., Herrmann, H., Worsnop, D. R., Kulmala, M., Kerminen, V.-M., and Petäjä, T.: Reactivity of stabilized Criegee intermediates (sCIs) from isoprene and monoterpene ozonolysis toward SO2 and organic acids, Atmos. Chem. Phys., 14, 12143-12153, doi:10.5194/acp-14-12143-2014, 2014.

Spracklen, D. V. and Heald, C. L.: The contribution of fungal spores and bacteria to regional and global aerosol number and ice nucleation immersion freezing rates, Atmos. Chem. Phys., 14, 9051-9059, doi:10.5194/acp-14-9051-2014, 2014.

Thonicke, K., Venevsky, S., Sitch, S., and Cramer, W.: The role of fire disturbance for global vegetation dynamics: Coupling fire into a dynamic global vegetation model, Global Ecology and Biogeography, 10, 661-677, 2001.

Thonicke, K., Spessa, A., Prentice, I. C., Harrison, S. P., Dong, L., and Carmona-Moreno, C.: The influence of vegetation, fire spread and fire behaviour on biomass burning and trace gas emissions: Results from a process-based model, Biogeosciences, 7, 1991-2011, 10.5194/bg-7-1991-2010, 2010.

van der Werf, G. R., Randerson, J. T., Giglio, L., Collatz, G. J., Mu, M., Kasibhatla, P. S., Morton, D. C., DeFries, R. S., Jin, Y., and van Leeuwen, T. T.: Global fire emissions and the contribution of deforestation, savanna, forest, agricultural, and peat fires (1997-2009), Atmos. Chem. Phys., 10, 11707-11735, DOI 10.5194/acp-10-11707-2010, 2010.

Veira, A., Kloster, S., Wilkenskjeld, S., and Remy, S.: Fire emission heights in the climate system–part 1: Global plume height patterns simulated by echam6-ham2, Atmospheric Chemistry and Physics Discussions, 15, 6645-6693, 2015.

Wang, Y., X. Liu, C. Hoose, and B. Wang, 2014: Different contact angle distributions for heterogeneous ice nucleation in the Community Atmospheric Model version 5. Atmos. Chem. Phys., 14, 10411-10430.

Changes with respect to the DoW

No changes with respect to the DoW.

Dissemination and uptake

The developed models will be used in WP4 tasks 4.3, 4.4 and 4.5.